ABSTRACT

Non-Contact Measurement for Thermal Conductivity of Diamond-Like and Hard Carbon Thin Films

by
Ganming Qin

In this research work, non-contact temperature measurement was applied to determine the thermal conductivity of diamond-like and hard carbon thin films. Dielectric materials widely used as thin films in device manufacturing are SiO_2, Si_3N_4, polymer, and etc. However, their heat dissipating capacity is not good for power devices. It is necessary to develop a new material for this purpose. Diamond crystal is a high quality dielectric material. It has the highest room-temperature thermal conductivity [$k=20 W/(cm \cdot K)$ at 20°C] among all materials. In addition, it has high electrical resistivity ($>10^{16}\ \Omega \cdot cm$) and high strength [1]. So, diamond-like film is the first candidate for this purpose. Two methods were reported to measure the thermal conductivity of diamond-like films [2, 3]: a DC technique [4] and an AC (or 3ω) technique [5,6]. In these methods, the temperature was measured by thermocouple or thermal resistor. The accuracy of the measurement will be affected by the leads of the sensors, since thermal energy will be transferred through the lead wires. This restricts the technique samples of thickness ≥ 5 μm. In practice, the thickness of diamond-like films used in power device applications is about 1 μm or even less. In our experiment, contactless temperature measurement for thermal conductivity of diamond-like and hard carbon thin films was introduced to measure the samples with thickness of 2μm. The experimental results show that this

method is useful to study thermal conductivity of diamond-like and hard carbon thin films. In the thesis, fundamentals of thermal detection are reviewed; the design, procedure, and validity of non-contact measurement method are presented; and experimental results are reported and discussed.

NON-CONTACT MEASUREMENT FOR THERMAL CONDUCTIVITY OF DIAMOND-LIKE AND HARD CARBON THIN FILMS

by
Ganming Qin

A Thesis
Submitted to the Faculty of
New Jersey Institute of Technology
in Partial Fulfillment of the Requirements for the Degree of
Master of Applied Physics

Department of Physics

May 1993

APPROVAL PAGE

Non-Contact Measurement for Thermal Conductivity of Diamond-Like and Hard Carbon Thin Films

Ganming Qin

Feb. 4, 93

Dr. K. Ken Chin, Thesis Advisor (Date)
Professor
Department of Physics
New Jersey Institute of Technology

2/4/93

Dr. J. C. Hensel, Committee Member (Date)
Distinguished Research Professor
Department of Physics
New Jersey Institute of Technology

2/4/93

Dr. Eugene J. Gordon, Committee Member (Date)
Distinguished Professor
Department of Electrical and Computer Engineering
New Jersey Institute of Technology

BIOGRAPHICAL SKETCH

Author: Ganming Qin

Degree: Master of Science in Applied Physics

Date: May 1993

Date of Birth:

Place of Birth:

Undergraduate and Graduate Education:

- Master of Applied Physics
  New Jersey Institute of Technology, Newark, NJ, 1993

- Master of Science in Physics
  South China University of Technology, Guangzhou, 1986

- Bachelor of Science in Physics
  South China University of Technology, Guangzhou, 1978

ACKNOWLEDGMENT

The author would like to express his gratitude to his advisor Dr. K. Ken Chin for his support, guidance and great help during the thesis research.

The author would also like to thank Dr. J. C. Hensel for his helpful discussions in the research and for his guidance in the use of measurement apparatus.

Special thanks to Professor Eugene I. Gordon for serving as a member of the committee and giving me very helpful suggestions on the thesis.

Professor Guanhua Feng participated in part of the research work. The author appreciates his contribution. The author has gotten a lot of help during his study and research work from many people in the Department of Physics, NJIT. The author wishes to thank all of them.

This work was partly supported by an NSF grant(#ESC-9114824) and a grant from the Center for Manufacturing System, which is sponsored by New Jersey Commission on Science and Technology.

TABLE OF CONTENTS

Chapter **Page**

LIST OF FIGURES

Figure **Page**

CHAPTER 1
INTRODUCTION

In this work, an accurate technique for the measurement of the thermal conductivity of diamond-like and hard carbon thin films used in semiconductor devices was introduced. The synthesis of crystalline diamond dates back to early this century. In 1911, Von Bolton claimed to have achieved growth of diamond seed crystals from decomposition of illuminating gas (C_2H_2) in the presence of Hg vapor. Subsequently, synthesis of hard and dense forms of carbon was reported, using simple thermal deposition of carbon containing gases, such as CB_4/CCl_4 and CH_4 . These methods have low growth rates and other problems. Recently, considerable interest has been aroused in the synthesis of diamond-like and hard carbon thin films using plasma assisted chemical vapor deposition (CVD) as well as physical vapor deposition (CVD) techniques. They are widely used as coating for microelectronic and optoelectronic devices, as well as other industrial products. Several parameters of diamond-like and hard carbon thin films such as thermal conductivity, hardness, and electrical resistivity, are better than those of other widely used materials such as SiO_2 and Si_3N_4. For example, due to high thermal conductivity, the diamond-like and hard carbon thin films are used as contacts to heat sinks for high power lasers, high power transistors, high power IMPATTs. Thermal conductivity of diamond-like and hard carbon thin film is an important characteristic. Two methods [2,3] are reported to determine the thermal conductivity of the diamond-like film: a DC (the standard steady-state four-probe measurement) technique [4] and an AC (or "3ω") technique [5,6].

The DC technique can be described as follows: A heater was made of a metal film evaporated on the surface of one end of a substrate, And a resistance thermometer or a thermocouple was attached to the surface of the center part of the sample. The other end of the sample was clamped to the heat sink with a copper clamp using indium as a cushion. This heater was used to generate a temperature difference ΔT across the film. For a heater power P, the thermal conductivity k of the film is given by $k = \frac{P \cdot l}{\Delta T \cdot A}$, where A is the cross-sectional area of the film and l the distance across which ΔT is generated. This temperature difference was detected using the thermometer.

The principle of the AC technique can be explained briefly as follows [5,6]. One end of the sample is periodically heated, and the temperature amplitude (this is defined as AC temperature, T_{AC}) at the point apart from the heated area by distance x is monitored with a thermocouple directly attached to the sample surface. The relation between AC temperature and distance x is given by the equation, $\ln|T_{AC}| = \ln\frac{q}{4\pi f Cd} - \frac{\pi f}{k}x$, where q is heat quantity absorbed by the sample, f is heating frequency, and C, d, and k are the specific heat, thickness, and thermal conductivity of the sample, respectively. Thus thermal conductivity can be evaluated from the slope of the equation by varying distance x.

In Reference [2], the authors used these two methods to determine the thermal conductivity of diamond-like film with thickness of 170 μm. In Reference [3], the authors measured the thermal conductivity of two films using dc technique. The thickness of these films was 18 and 13 μm,

respectively. In their experiments, the films were peeled from their substrates. In Reference [7], authors claimed to use 3ω method to measure the thermal conductivity of a 5-μm-thick diamond-like film on the Si substrate (about 100-μm thick).

In these two methods, of crucial importance is whether any heat lost via other heat-transfer mechanisms such as radiation, conduction and convection of the air, and conduction through the heater and detector wire leads. Furthermore, as limitation of these methods, it is difficult to measure the thermal conductivity of thinner films (with thickness less than 1 μm) by these methods. In these methods, the sample temperature was measured by a thermocouple or thermistor sensor which had to be contacted to the sample. So, the loss of the heat through the sensor leads will affect the result of the measurement. This influence is serious if the thickness of samples is less than 2 μm.

In our experiment, we introduce a non-contact method to measure thermal conductivity of diamond-like and hard carbon thin films: non-contact temperature measurement by which we can measure the sample as thin as 2μm. The error by the conduction through wires is eliminated by this method. The radiation was taken into account in the experimental analysis. The conduction and convection through the gas was made negligible by using a vacuum system with 10^{-5} Torr pressure.

CHAPTER 2
PRINCIPLES OF NON-CONTACT MEASUREMENT OF THERMAL DETECTION

2.1 Configuration of Non-Contact Measurement of Thermal Conductivity

The system for measuring lateral thermal conductivity of a diamond-like or hard carbon thin film with a thickness as small as 1-2 μm was designed as shown in Figure 1.

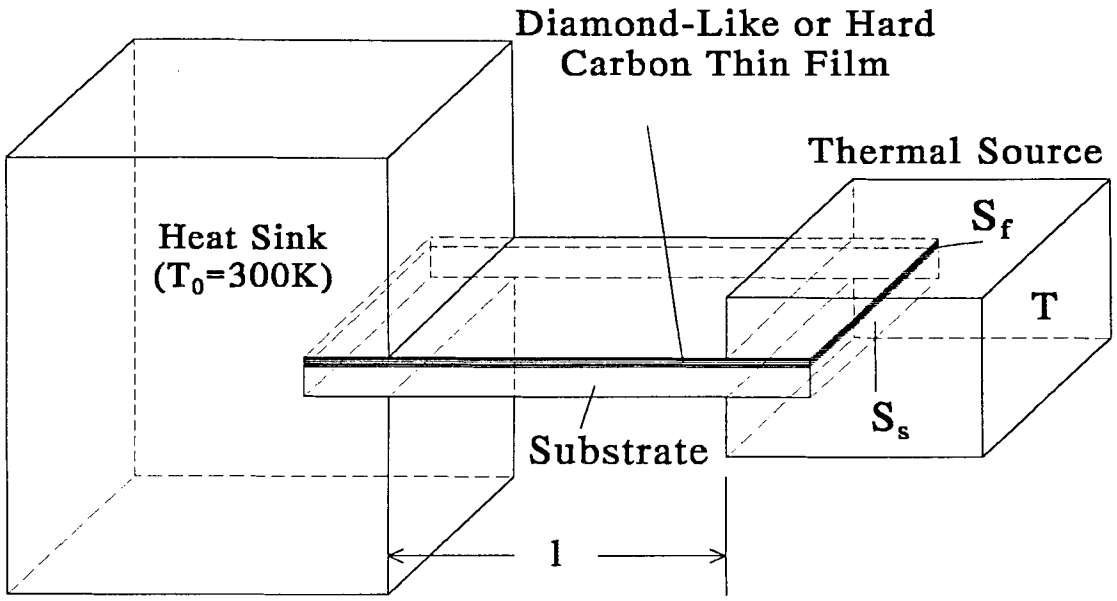

Figure 1 Configuration of Experimental Sample

In the experiment, the glass substrate coated with diamond-like or hard carbon thin film was connected between the source and sink. The source consisted of an aluminum plate with blackened surface. The temperature was detected by the radiation of the source. The thermal sink was a large block of copper of sufficient heat capacity so that the temperature of the sink keeps almost at room temperature. If the thermal source is heated to above room temperature $\Delta T_0 = (T - T_0)$ and then heating is stopped, the thermal energy of the source will go out by radiation, conduction through the diamond-like or hard carbon film and the glass substrate, and convection through gas. At the same time, the temperature of the thermal source drops, i.e.,

$$\begin{aligned} -C\frac{d\Delta T}{dt} &= k_f \frac{S_f}{l_f}(T - T_0) + k_s \frac{S_s}{l_s}(T - T_0) \\ &\quad + \varepsilon A\,\sigma(T^4 - T_0^4) + k_g \frac{S_g}{l_g}(T - T_0) \\ &= P_1 + P_2 + P_3 + P_4 \end{aligned} \tag{1}$$

where C is the heat capacity of the source:

$$C = \rho \cdot V \cdot c \tag{2}$$

where ρ is the density of the Al. V is the volume of the source. c is the specific heat of Al[c = 0.83 J/(g• K)]. On the right hand side of Equation (1), the terms representing heat loss are the followings:

P_1 is the thermal energy flux flowing from the heat source to the heat sink through the diamond-like film.

$$P_1 = K_f (T - T_0) \tag{3}$$

$$K_f = k_f \frac{S_f}{l_f} \tag{4}$$

where S_f is the cross-sectional area of the films, l_f is its length and K_f is its thermal conductivity.

P_2 is the thermal energy flux flowing from the source to the heat sink through the glass Substrate.

$$P_2 = K_s (T - T_0) \tag{5}$$

$$K_s = k_s \frac{S_s}{l_s} \tag{6}$$

where S_s is the cross-sectional area of the films, l_s is its length and K_s is its thermal conductivity.

P_3 is the thermal energy radiating from the source to the surrounding.

$$P_3 = \varepsilon A \sigma (T^4 - T_0^4) \tag{7}$$

where ε is the emissivity of the thermal object, A is the surface area of the object, and σ is Stefan-Boltzmann constant. For $T - T_0 << T$,

$$(T^4 - T_0^4) \approx 4T^3 (T - T_0) \tag{8}$$

Thus, we may approximate P_3 by

$$P_3 \approx \varepsilon A \sigma 4 T^3 (T - T_0) = K_r (T - T_0) \tag{9}$$

K_r is the radiation constant of the heat source:

$$K_r = 4 \varepsilon \sigma A T^3 \tag{10}$$

P_4 is the thermal energy dissipated through the gas in the vacuum system due to the thermal conductivity of the gas [8].

$$P_4 = k_g \frac{S_g}{l_g} (T - T_0) \tag{11}$$

where S_g is the area of surfaces facing each other. l_g the distance between surfaces. k_g the thermal conductivity of the gas: $k_g = k_g^{'} \cdot p$, where p is the gas pressure. For air, $k_g^{'} = 0.24 \times 10^{-3} \, \mathrm{W/(cm \cdot K \cdot Torr)}$ [8]. In this experiment, pressure of vacuum system= 10^{-5} τ. k_g will be about $0.24 \times 10^{-8} \, \mathrm{W/(cm \cdot K)}$. Compared with P_1, P_2 and P_3, P_4 which is due to the gas conduction, can be neglected.

From Equation (1), we can write in brief:

$$-C \frac{d\Delta T}{dt} = K \Delta T \tag{12}$$

where $K = K_f + K_s + K_r$ (13)

The solution of the above differential equation is:

$$\Delta T = (\Delta T)_{t=0} e^{-t/\tau} \tag{14}$$

$$\text{where } \tau = \frac{C}{K} = \frac{C}{K_f + K_s + K_r} \tag{15}$$

τ is the time constant:

$$\tau^{-1} = \tau_f^{-1} + \tau_s^{-1} + \tau_r^{-1} \tag{16}$$

$$\tau_f^{-1} = \frac{K_f}{C} \tag{17}$$

$$\tau_s^{-1} = \frac{K_s}{C} \tag{18}$$

$$\tau_r^{-1} = \frac{K_r}{C} \tag{19}$$

To extract K_f from the experiment, we plot Equation (14) in semi-log scale:

$$\log \Delta T = \log(\Delta T)_{t=0} - \frac{C}{K} t \tag{20}$$

From the slope we get $-\frac{C}{K}$. So, K is given as:

$$K = K_f + K_s + K_r = -\frac{C}{slope} \tag{21}$$

Now if we measure the thermal conductivity of the substrate without diamond-like film on, the effective conductance becomes

$$K' = K_s + K_r - \frac{C}{slope'} \tag{22}$$

And finally, if we measure the thermal conductivity of the substrate with diamond-like film on, the effective conductance becomes

$$K'' = K_f + K_s + K_r = -\frac{C}{slope''} \tag{23}$$

So, the thermal conductance of the diamond-like or hard carbon thin film is:

$$K_f = K'' - K' = \frac{C}{slope'} - \frac{C}{slope''} \tag{24}$$

2.2 Limitations of the Experiment

The thermal source is made of Al with 0.60x0.60x0.16cm^3. It was blackened to make the emissivity is as high as possible (emissitivity ε is about 0.85). Thus,

$$\begin{aligned} K_r &= 4\varepsilon\sigma A T^3 \\ &= 4 \times 0.85 \times 5.67 \times 10^{-12} \times 1.104 \times 330^3 \\ &= 7.6 \times 10^{-4} \qquad (\mathrm{K/W}) \end{aligned} \tag{25}$$

A glass plate was used as a substrate. The length l is equal to 0.20cm, the width w is equal to 0.60cm, and the thickness t is equal to 200 μm. From Reference [9], the thermal conductivity of glass is:

$$k \approx 8 \times 10^{-3} \qquad [\mathrm{W}/(\mathrm{cm}\cdot\mathrm{K})] \tag{26}$$

Thus,

$$\begin{aligned} K_S &= k_S \frac{S_s}{l_s} = 8 \times 10^{-3} \times \frac{0.6 \times 0.02}{0.2} \\ &= 4.8 \times 10^{-4} \qquad (\mathrm{W}/\mathrm{K}) \end{aligned} \tag{27}$$

The thermal conductivity of the hard carbon thin film ranges from 0.02 to 10[W/(cm·K)][3]. Assume that the thickness is 2μm and $k_f = 0.1[\mathrm{W}/(\mathrm{cm}\cdot\mathrm{K})]$, then K_s is given by:

$$\begin{aligned} K_f &= k_f \frac{S_f}{l_f} = 0.1 \times \frac{0.6 \times 0.002}{0.2} \\ &= 6 \times 10^{-4} \qquad (\mathrm{W}/\mathrm{K}) \end{aligned} \tag{28}$$

From the above data calculated, we note that these values are almost the same order. We can easily separate the K_f of the diamond-like and hard carbon thin films from the experiment data. To improve the experiment accuracy, we should reduce the dimension of the thermal source and the thickness of the substrate so that K_r and K_s is very small compared with K_f. If all dimensions including the thickness of the film are reduced by half, then,

$$\begin{aligned} K_r &= 4\varepsilon\sigma A T^3 \\ &= 4 \times 0.85 \times 5.67 \times 10^{-12} \times 0.276 \times 330^3 \\ &= 1.91 \times 10^{-4} \qquad (\mathrm{K}/\mathrm{W}) \end{aligned} \tag{29}$$

$$K_s = k_s \frac{S_s}{l_s} = 8 \times 10^{-3} \times \frac{0.3 \times 0.01}{0.1} \\ = 2.4 \times 10^{-4} \quad (\mathrm{W/K}) \tag{30}$$

$$K_f = k_f \frac{S_f}{l_f} = 0.1 \times \frac{0.3 \times 0.001}{0.1} \\ = 3 \times 10^{-4} \quad (\mathrm{W/K}) \tag{31}$$

In this case, K_f is Larger than K_r and K_s. That is to say, we can measure the thermal conductivity of diamond-like and hard carbon thin films of 1-μm thickness. Reducing the dimension of the source is limited by the detectivity of the detection system including detector, preamplifier, and lock-in amplifier. Next sections, we will review the basic concepts of thermal detection and testing.

2.3 Infrared Radiation

Planck's Law for Spectral Exitance at temperature T is(see Figure 2) :

$$M(\lambda, T) = \frac{2\pi hc}{\lambda^5 (e^{\frac{hc}{k_B \lambda T}} - 1)}$$

$$= \frac{3.7417749 \times 10^4}{\lambda^5 (e^{\frac{14387.69}{\lambda T}} - 1)} \quad [\mathrm{W/(cm^2 \mu m)}] \tag{32}$$

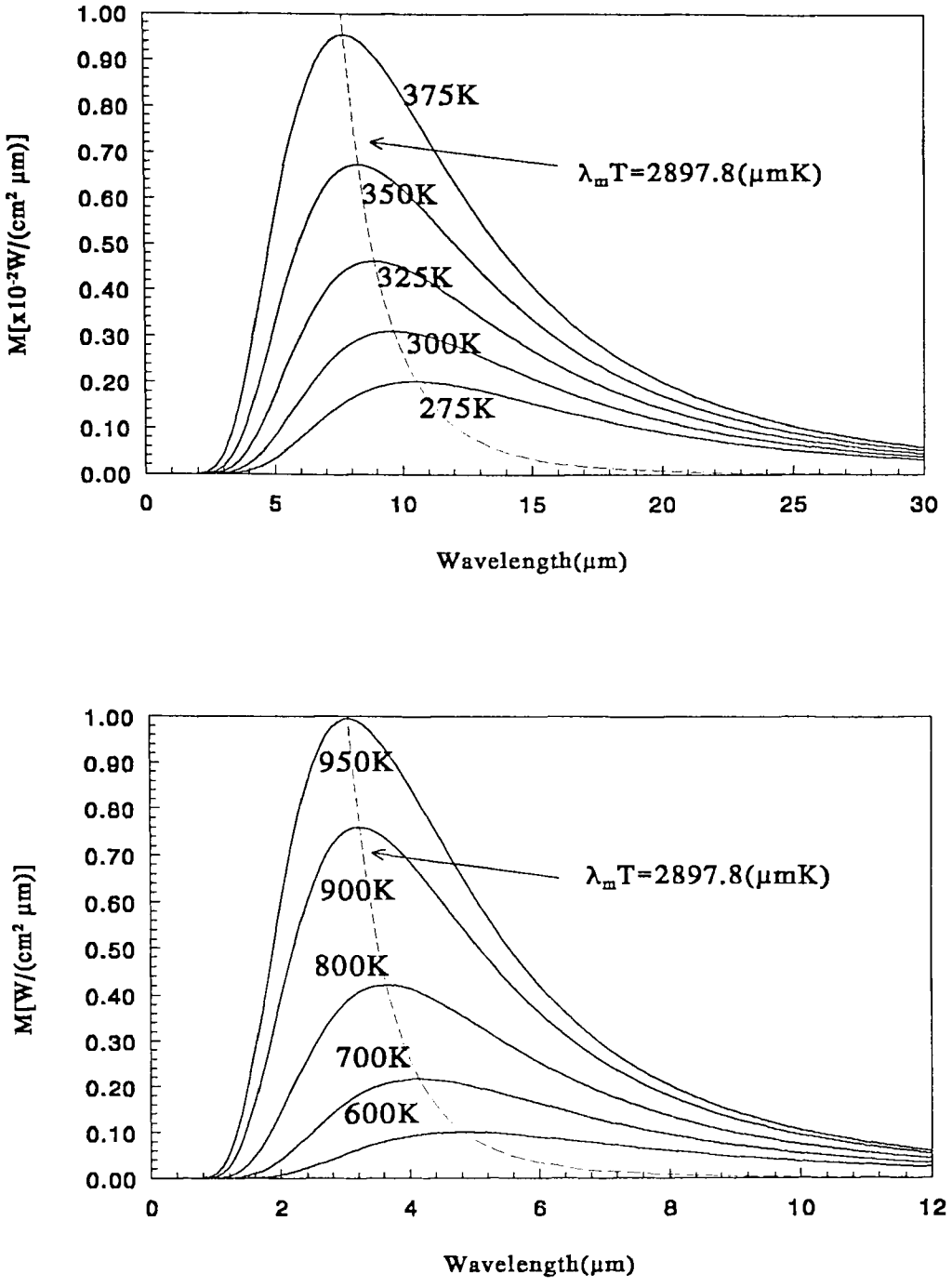

Figure 2 Planck's Law: Spectral Exitance vs. Wavelength

where $M(\lambda,T)$ is radiant exitance defined as the radiation power into a hemisphere per unit emitter area of the ideal blackbody and per unit wavelength at wavelength λ, h is Plank's constant, c the speed of light in the vacuum, k_B Boltzmann's constant, and T the temperature of the blackbody radiation.

Planck's Law for Total Blackbody Exitance at temperature T gives Stefan's Law:

$$M(T) = \int_0^\infty M(\lambda,T)d\lambda = \sigma T^4 \qquad [\mathrm{W/cm^2}] \tag{33}$$

where σ is Stefan-Boltzmann constant

$$\sigma = 5.67051 \times 10^{-12} \qquad \mathrm{W/(cm^2 \cdot K^4)} \tag{34}$$

At about room temperature, 80 percent of the total radiation power is concentrated in the wavelength range between 6.5-30 μm.

2.4 Incremental Power Transfer

In the incremental limit, consider the power transferred between two very small surface areas of source and detector, as shown in Figure 3. The incremental power transfer is [8]:

$$P = \frac{(\varepsilon \Delta A_S \cdot \cos\theta_S)(\alpha \Delta A_d \cdot \cos\theta_d)}{\pi r^2} \tau M(\lambda,T) \qquad [\mathrm{W}] \tag{35}$$

where ΔA_S and ΔA_d are incremental areas of the thermal source and the detector, respectively. r is the distance between ΔA_S and ΔA_d. θ_S and θ_d are

the angles between the line connecting two surfaces and the normal of the source surface , and that of the detector surface, respectively. τ is the composite transmittance between the source and detector. In our experiment no optical components are put in the way of the path, and therefore, $\tau = 1$.

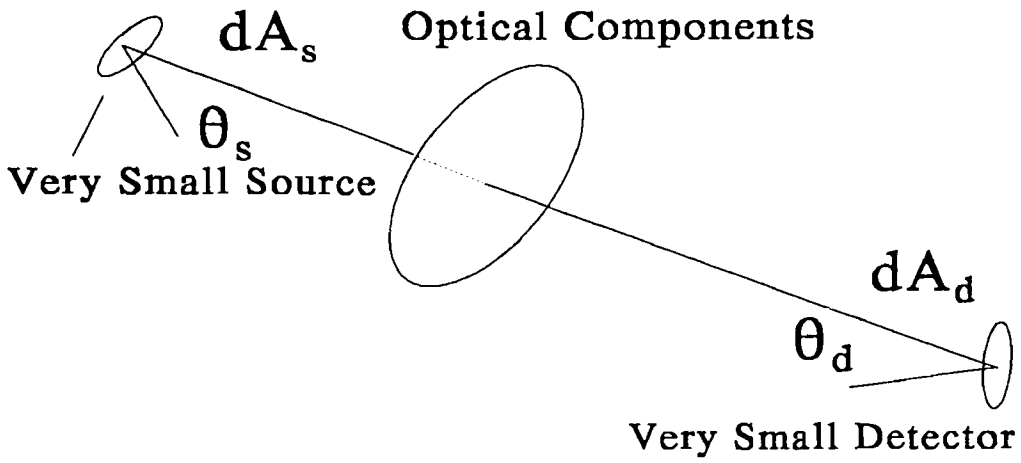

Figure 3 Incremental Power Transfer of Two Surfaces

2.5 Non-Contact Temperature Measurement

The design of the non-contact temperature measurement experiment is shown in Figure 4. A pyroelectric detector is used so that no detector cooling is needed. To avoid background noise in a non-contact measurement, a beam aperture of small radius is needed. As the source and the detector face each other directly, the radiation power P falling on the detector is [8]:

$$P = \varepsilon \sigma T^4 \cdot (\pi r_d^2) \cdot \frac{r_a^2}{R^2 + r_a^2} \tag{36}$$

where r_d is the radius of the detector. r_a is the radius of the defining aperture. r_a should be small enough to well confine the thermal source from the background. The radius of the spot on the thermal source seen from the detector is:

$$\begin{aligned} r_s &= r_a + \frac{b}{R} \cdot r_d \\ &= 0.11 + \frac{1.7}{5.35} \times 0.1 = 0.142 \qquad \text{(cm)} \end{aligned} \tag{37}$$

The area of the thermal source facing the detector is $0.60 \times 0.6 cm^2$. So, the confining aperture is small enough for the experiment.

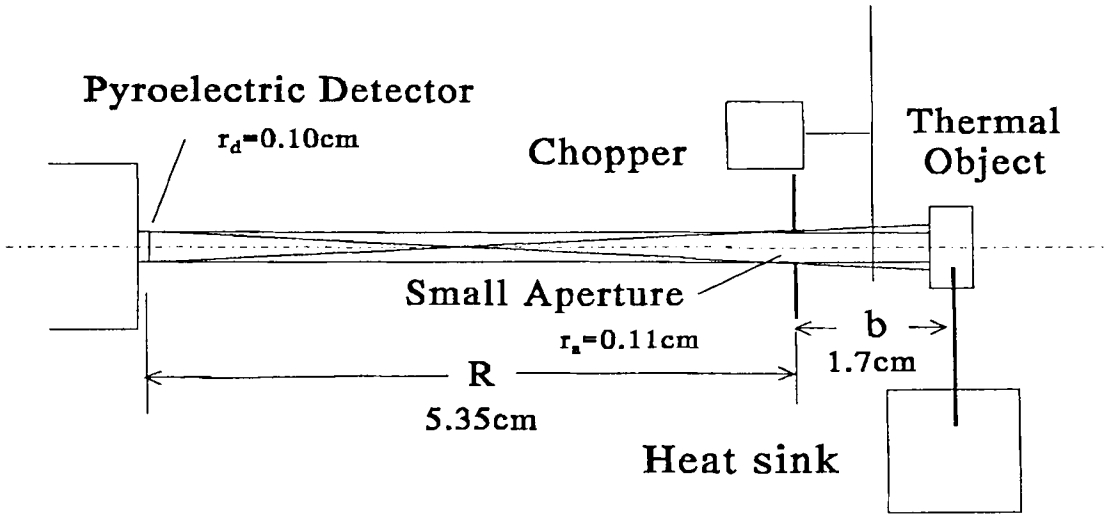

Figure 4 Non-Contact Measurement of Thermal Conductivity of Thin Films

To reduce *1/f* and other noises, a chopper and a lock-in amplifier is often used in IR detection. For a pyroelectric detector, it is the change of the incidence of the instrument measures. So the chopping of the radiation signal from an object is necessary. Any periodic waveform can be written mathematically as a Fourier series, or the sum of a number of sinusoidal waves. We are interested in the first term (fundamental component). its frequency is the fundamental frequency which is the same as that of the arbitrary waveform. We define the modulation factor as:

$$\mathrm{MF} = \frac{\text{rms value of fundamental component}}{\text{peak - to - peak value of total waveform}} \tag{38}$$

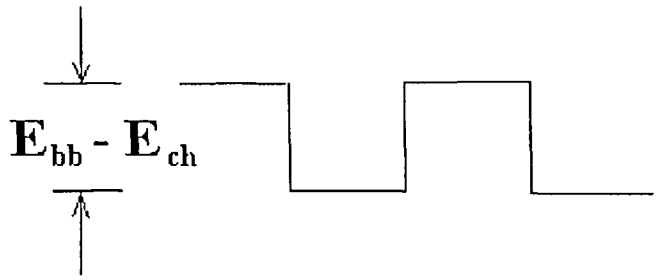

Figure 5 Modulated Incidence from a Thermal Source.

A large toothed chopper moving past a very small aperture yields very nearly a square wave. For square waveform, $\mathrm{MF} = \frac{\sqrt{2}}{\pi} \cong 0.45$.

The chopper is mounted between the aperture and the thermal source, so as the chopper rotates, the detector sees no changes except through the aperture. Thus the difference between the maximum incidence and the minimum incidence is just the incidence from the thermal source less that from the room-temperature chopper, both viewed through the same projected solid angle of the aperture from the detector. The power difference between the thermal source and background falling on the detector is (Figure 5):

$$\Delta P = \varepsilon \sigma (T^4 - T_0^4) \cdot (\pi r_d^2) \cdot \frac{r_a^2}{R^2 + r_a^2} \cdot \mathrm{MF} \tag{39}$$

2.6 Detector Parameters and Definitions

The following parameters are defined to characterize the detector and detection system.

- Responsivity(R)

Responsivity is the characteristic of the detection system responding to the incidence. It is defined as:

$$R(\mathrm{V/W}) = \frac{\text{signal output voltage}}{\text{IR input power}} = \frac{S(\mathrm{V})}{E(\mathrm{W/cm^2}) \cdot A_d(\mathrm{cm^2})} \tag{40}$$

- Noise(N)

Noise is caused by random thermal motion of carriers, and photons which do not arrive at an absolutely constant rate (the arrival rate fluctuates slightly). This kind of noise is unavoidable. There is another kind of noise which is avoidable. It includes: electrical interference such as motor, ac power lines, detector temperature fluctuations, and vibrations that cause electrical components to shift.

Since noise is a random deviation from the average of the signal, the root-mean-square (rms) deviation is used to describe the noise. From frequency spectrum of noise of a typical detector (as shown in Figure 6) [8], we can see that there is white noise which is almost uniform at all frequencies. Interference noise is at very specific frequencies caused by mechanical vibration, power lines and etc. $1/f$ noise increases greatly as the frequency goes down. For white noise, it is found that the total noise voltage in the band (Δf) is proportional to $\sqrt{\Delta f}$. In general, we define noise spectral density as:

$$n(\mathrm{V}/\mathrm{Hz}^{1/2}) = \frac{N(\mathrm{V})}{\sqrt{\Delta f(\mathrm{Hz})}} \tag{41}$$

The interference noise and the $1/f$ noise are important in thermal detection because the time responsivity of thermal detectors is usually slow. The working frequency of detector is about several Hz to several hundred Hz.

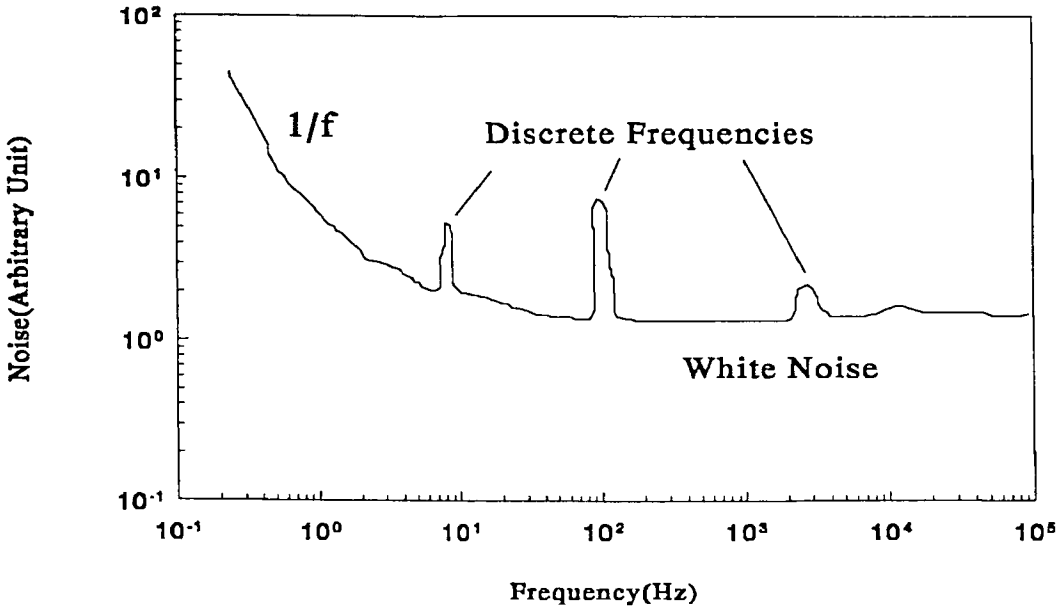

Figure 6 Frequency Spectrum of Noise of a Typical Detector.

- Signal-to-Noise Ratio(*S/N*)

S/N describes how much the incidence overcomes the noise. If the incidence signal is smaller than the noise(*S/N*<1), we can not tell the signal from the noise. Usually, we should enhance the incidence or decrease the noise of the detector so that *S/N* > 30.

- Noise Equivalent Power(*NEP*)

NEP is a measure of the ultimate sensitivity of a given detector. *NEP* is the power that must fall on the detector to cause an *S/N* of 1. It is determined by dividing the system noise by the responsivity(*R*):

$$NEP(\mathrm{W}) \equiv \frac{N(\mathrm{V})}{R(\mathrm{V/W})} = \frac{N(\mathrm{V}) \cdot E(\mathrm{W/cm^2}) \cdot A_d(\mathrm{cm^2})}{S(\mathrm{V})} \tag{42}$$

- Detectivity(*D*)

Detectivity of a Detector is Defined as:

$$\begin{aligned} D(1/\mathrm{W}) &\equiv \frac{1}{NEP(\mathrm{W})} = \frac{R(\mathrm{V/W})}{N(\mathrm{V})} \\ &= \frac{S(\mathrm{V})}{N(\mathrm{V}) \cdot E(\mathrm{W/cm^2}) \cdot A_d(\mathrm{cm^2})} \end{aligned} \tag{43}$$

A good detector should have a small *NEP*. The greater the detectivity *D* of the detector, the smaller the irradiance we can measure. Detectors of different sizes will have different detectivity. Extensive theoretical and experimental studies have shown that it is reasonable to assume that detectivity varies inversely as the square root of the area of the detector, i.e.,

$$D \propto \frac{1}{\sqrt{A_d}} \tag{44}$$

Notice that *NEP* is proportional to the square root of the band-width. So it is convenient to introduce the quality specific detectivity (D^*) (normally called detectivity or D-star"), which is independent of the bandwidth and detector size, referred to a post-detector amplifier bandwidth of 1Hz and a detector area of 1 cm^2.

$$\begin{aligned} D^*(\mathrm{cm}\cdot\mathrm{Hz}^{1/2}/\mathrm{W}) &= \frac{1}{NEP(\mathrm{W})}\cdot\sqrt{A_d(\mathrm{cm}^2)}\cdot\sqrt{\Delta f(\mathrm{Hz})} \\ &= \frac{S(\mathrm{V})\cdot\sqrt{\Delta f(\mathrm{Hz})}}{N(\mathrm{V})\cdot E(\mathrm{W}/\mathrm{cm}^2)\cdot\sqrt{A_d(\mathrm{cm}^2)}} \end{aligned} \tag{45}$$

D^* is useful in predicting *S/N* in a given test environment.

$$S/N = D^*(\mathrm{cm}\cdot\mathrm{Hz}^{1/2}/\mathrm{W})\frac{E(\mathrm{W}/\mathrm{cm}^2)\cdot\sqrt{A_d(\mathrm{cm}^2)}}{\sqrt{\Delta f(\mathrm{HZ})}} \tag{46}$$

- Time Response of detector

For thermal type of detectors, time constant τ of detector is the product of the thermal impedance of its mounting structure and the heat capacity of the sensor. It ranges from 1 millisecond to 1 second. The responsive speed of photo-detectors is faster than that of thermal detector.

- Spectral Response

By spectral response we mean how the responsivity of the detector varies with the wavelength of the detected radiation.

CHAPTER 3
EXPERIMENTAL SYSTEM

The measuremental system is shown in Figure 7. It includes a sample holder, a heat source, a heat sink, a thermal detector, a chopper, a chopper control box, a lock-in amplifier, and the computer data acquisition system.

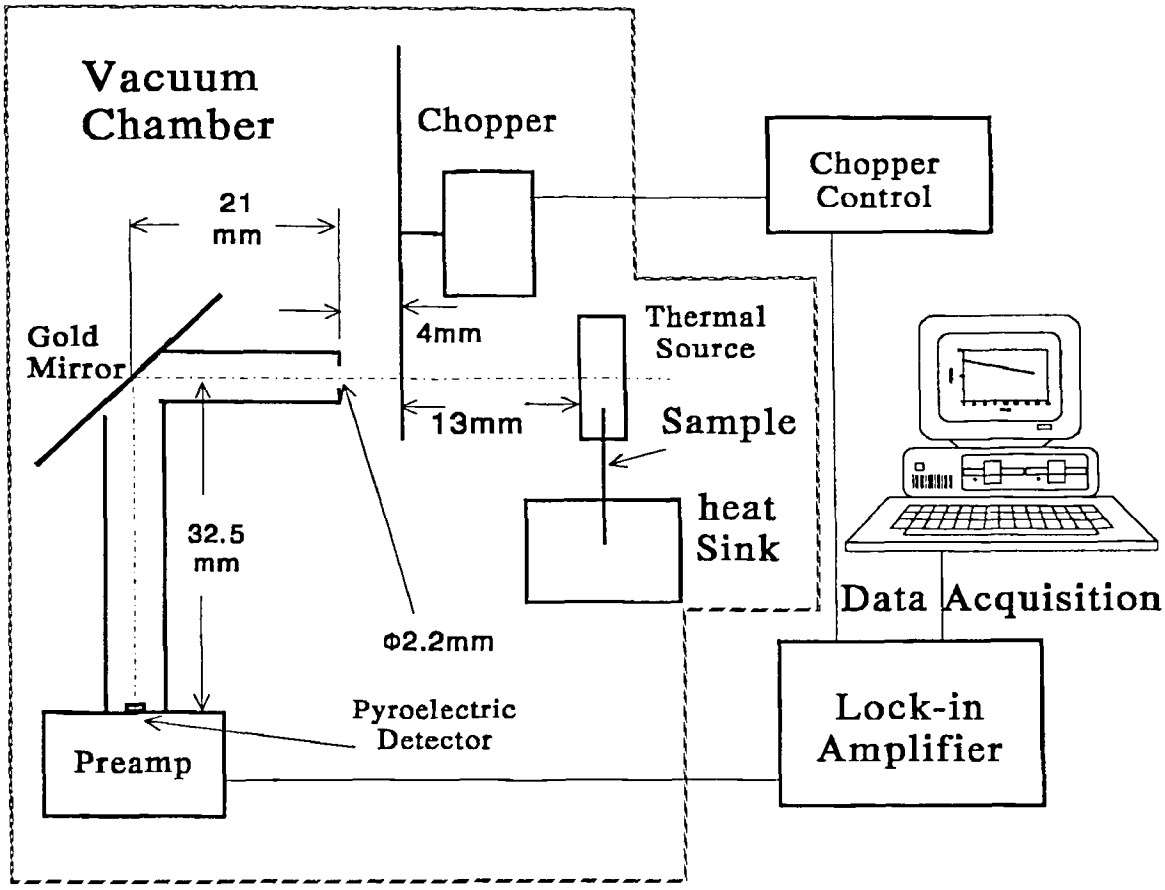

Figure 7 Block Diagram of Thin Film Thermal Conductivity Measurement

3.1 Detector

There are two types of thermal detectors: thermal (heat) detection type and photo detection type. The thermal detection type includes: thermo-expansion type such as golay or pneumatic detector, thermoconductive (TC) type such as golay, bolometer, thermovoltaic (TV) type such as thermopile, pyroelectric detector, and etc. The photo detection type includes: photoconductive (PC) type such as Ge:Au, HgCdTe, PbS, photovoltaic (PV) type such as InSb and HgCdTe, and etc.

A pyroelectric detector is used in this experiment due to the fact that it can work at room temperature, has high detectivity and can detect room temperature thermal radiation. The pyroelectric effect is exhibited by certain materials that possess a permanent electric polarization along a particular axis. Barium titanate ($BaTiO_3$), triglycine sulfate, lithium sulfate (Li_2SO_4), and lithium niobate ($LiNbO_3$) are examples. The polarization which is a result of the relative displacement of lattices of positive and negative ions. It is associated with an unstable vibrational mode of the crystal that is temperature dependent. Below a certain temperature (the Curie temperature), which is characteristic of a particular material, the crystal is permanently polarized, but the lattice displacement and hence the electric dipole moment change with temperature. Thus, if the crystal is irradiated with infrared radiation, the temperature and the dipole moment will respond. But the electric dipole moment is generally masked by free charges that accumulate on the surface to neutralize the bound charges of the polarized crystal and, as the dipole moment changes the surface free charge will tend to redistribute. However, the polarization responds quickly to temperature changes, but the free charges

cannot redistribute quickly and cannot maintain zero net charge. Thus in response to a temperature change caused by radiation, a voltage appears between the faces of the crystal normal to the axis of polarization. Because the pyroelectric detector responds only to the change of the incidence, a chopper or shutter must be used. The pyroelectric detector has high impedance. Therefore it was usually connected to an FET pre-amplifier. In this experiment, the detector model is P1-72CC including a pyroelectric detector and an FET preamplifier (Figure 8). Detector features are as follows:

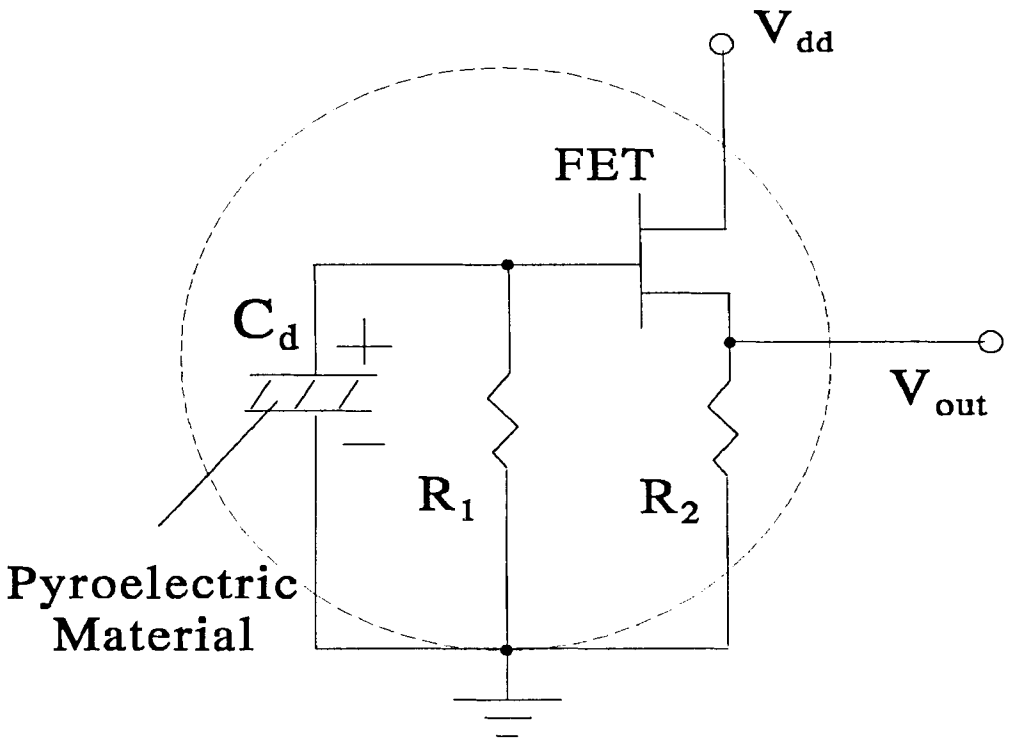

Figure 8 Ultra-Low Noise Pyroelectric Detector/FET Preamplifier.

- Rugged $LiTaO_3$ material
- 610°C Curie temperature
- 0.2 % /°C temperature stability
- Broad spectral range with wavelength from 0.001 to 1000 microns
- Low noise
- 0°C to 70°C operation
- Low leakage current hybrid FET preamplifier

The performance specifications(at 25°C) is as below:

d	Active Diameter	2 mm	
R_i	Current Responsivity of Element	.5 μA/W	λ=632.8nm, f=15Hz
R_v	Voltage Responsivity of Element/FET	432.0 V/W	λ=632.8nm, f=15Hz
		17.1V/W	λ=632.8nm, f=330Hz
N_v	Noise Voltage	.25 $\mu V/Hz^{1/2}$	λ=632.8nm, f=15Hz
		30 $\mu V/Hz^{1/2}$	λ=632.8nm, f=330Hz
NEP	Noise Equivalence Power	.58 $\times 10^{-9} W/Hz^{1/2}$	λ=632.8nm, f=15Hz
		1.8 $\times 10^{-9} W/Hz^{1/2}$	λ=632.8nm, f=330Hz
D^*	Detectivity	$3 \times 10^8 cm \cdot Hz^{1/2} / W$	λ=632.8nm, f=15Hz
		$.97 \times 10^8 cm \cdot Hz^{1/2} / W$	λ=632.8nm, f=330Hz
V_{dd}	Supply Voltage	+9V	

3.2 Lock-in Amplifier

The precision lock-in amplifier PAR Model HR-8 with a chopper and a chopper control is used. A lock-in amplifier is essentially a detection system capable of operating with an extremely narrow equivalent noise bandwidth. We know the noise is nearly proportional to the square root of the band. And the interfering signals can be suppressed by avoiding the operating frequency of lock-in system from that of interfering signals. The Lock-in is connected to the preamplifier of the detector.

3.3 Computer Data Acquisition

To make easy collection of data, we use a digital multimeter Keithley 190A connected to the lock-in amplifier of detection system and IBM 286 from Keithley 190A. The computer will record the voltage caused by the radiation as the function of the time. The computer program of the data acquisition is listed in Appendix A.

3.4 Sample Preparation

Plasma assisted chemical vapor deposition(PACVD) techniques are used for the synthesis of diamond-like or hard carbon coating on the substrate of thin glass. Diamond-like films were grown in the chamber of plasma CVD set up by our research group shown as in Figure 9. The reactive gas is methane(CH_4). The growing conditions are as follows:

Vacuum of System	1 mτ
Gas Flux	50 ml/min
Gas Working Pressure	100 mτ
Growing Temperature	180 °C
PF Power	75 W

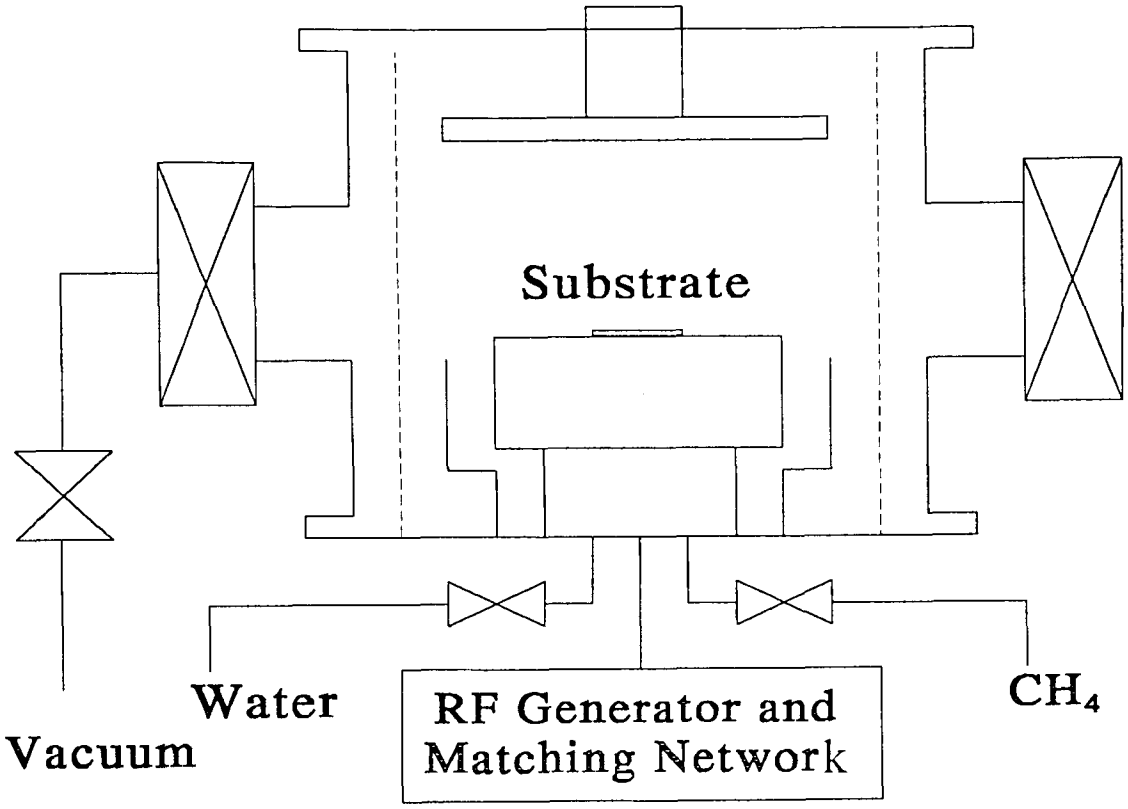

Figure 9 PACVD Growing System

Under these conditions, the growing rate was measured to be 2500 angstroms/hour. The refractive index of the film is about 1.8-2.0 measured by ellipsometer. This value is almost the same as the previous report[1]. The substrate is a glass plate of $1.2\times0.60\times cm^2$ with thickness 0.020 ± 0.002 cm. The hard carbon thin film was grown 8 hours to get the film as thick as 2 μm.

CHAPTER 4
EXPERIMENTAL RESULTS AND DISCUSSIONS

4.1 Calibration of the Pyroelectric Detector

In the vacuum chamber with mechanical and diffusion pumps, in which the pressure is as low as 10^{-5} Torr, a piece of Al of $0.60 \times 0.60 \times 0.16$ cm^3 with black coating was heated by a nearby transfer coil heater through radiation. After the thermal source is heated to a temperature of about 50°C above room temperature (300°K), we move the heater away by a rotator. The temperature of the thermal source will drop. The temperature was measured by a thermocouple in contact with the source. The chopper frequency is 17 Hz. The temperature vs. the voltage read out from the lock-in amplifier is plotted in Figure 10. The thermocouple is removed from the thermal source. The temperature of the thermal source was measured by the radiation incidence.

4.2 Radiation of the Thermal Source

The thermal source was hung by a very thin piece of paper of high thermal resistance. Radiation is the only mechanism of heat dissipation from the heat source in the vacuum chamber. Exponential function was used to fit the data plot. The coefficient — time constant τ of several tests are shown in Figure 11.

The average of τ_r^{-1} is:

$$\tau_r^{-1} = 0.00670 \text{s}^{-1} \tag{47}$$

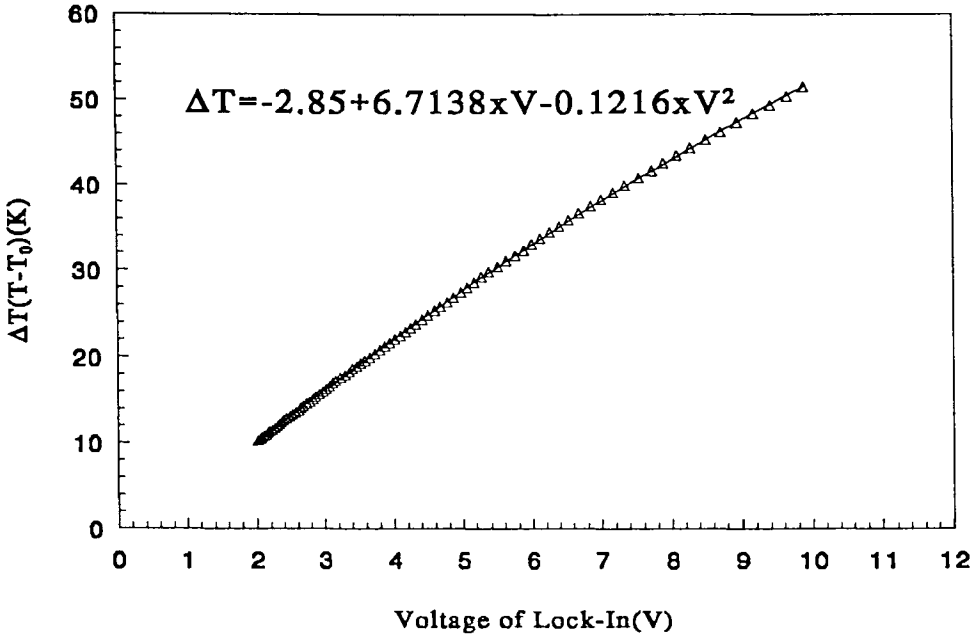

Figure 10 Calibration of the Pyroelectric Detector.

From Equation (19),

$$\begin{aligned} K_r &= \tau_r^{-1} \cdot C = 0.00670 \times 0.129 \\ &= 8.64 \times 10^{-4} \, (\text{K/W}) \end{aligned} \tag{48}$$

The result of the experiment is well concordant with that of theoretic analysis[see Equation (25)].

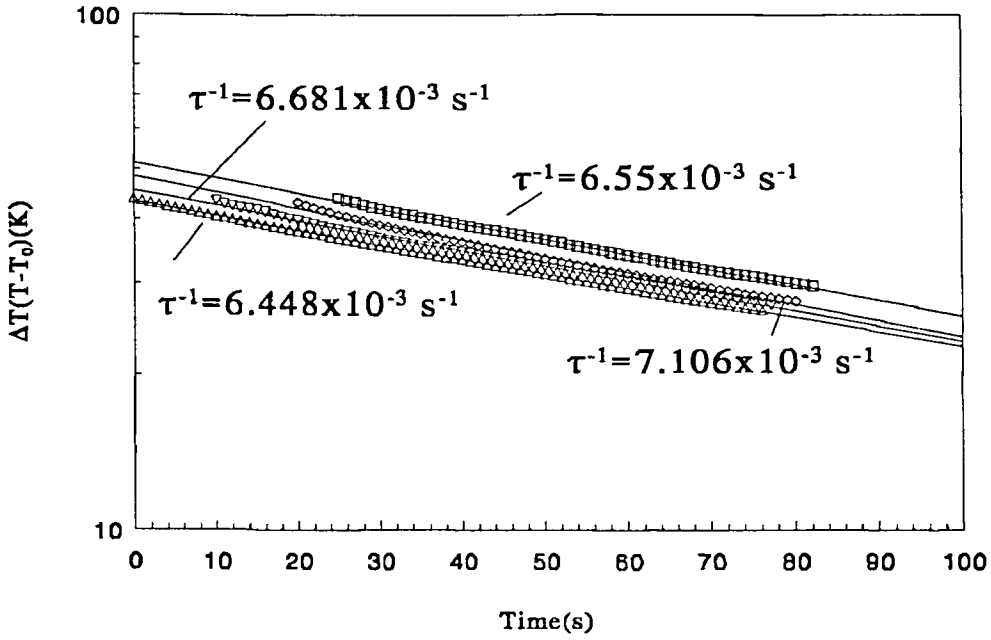

Figure 11 Temperature vs. Time due to Radiation.

4.3 Thermal Conductivity of Glass Plate

To test the validity of the principle, assumption, procedure, and equipment of the experiment, several glass plates of 1.2×0.60 cm^2 with thickness 0.020± 0.002 cm were served in the experiment. It is found that the temperature of the thermal source drops down faster than the case when the source was hung by a very thin piece of paper, since now the thermal energy transfers through both

radiation and conduction of the glass plate. From Figure 12, the average of $\tau^{-1}(=\tau_r^{-1}+\tau_s^{-1})$ of two tests is:

$$\tau^{-1}=0.010293\text{s}^{-1} \tag{49}$$

So,

$$\begin{aligned}\tau_s^{-1}&=\tau^{-1}-\tau_r^{-1}\\&=0.010293-0.00670=3.59\times10^{-3}(\text{s}^{-1})\end{aligned} \tag{50}$$

From Equations (6) and (18):

$$\begin{aligned}k_s&=\frac{Cl_s}{S_s}\tau_s^{-1}=\frac{.129\times.2}{.6\times.02}\times3.59\times10^{-3}\\&=7.72\times10^{-3}[\text{W}/(\text{cm}\cdot\text{K})]\end{aligned} \tag{51}$$

This value is in accord with the reference value of the bulk glass [9]. *This experimental result indicates the validity of this method.*

4.4 Thermal Conductivity of Hard Carbon Thin Film

Hard carbon thin films(with thickness of 2μm) were grown on some glass plates with dimensions as above. The experiment data of three tests are shown on Figure 13. The average of $\tau^{-1}(=\tau_r^{-1}+\tau_s^{-1}+\tau_f^{-1})$ is:

$$\tau^{-1}=0.010866\text{s}^{-1} \tag{52}$$

So,

$$\begin{aligned}\tau_f^{-1} &= \tau^{-1} - (\tau_r^{-1} + \tau_s^{-1}) \\ &= 0.010866 - 0.010293 \\ &= 5.73 \times 10^{-4} \qquad (s^{-1})\end{aligned} \tag{53}$$

From Equations (4) and (17):

$$\begin{aligned}k_f &= \frac{Cl_f}{S_f}\tau_f^{-1} = \frac{.129 \times .2}{.6 \times .0002} \times 5.73 \times 10^{-4} \\ &= 0.12 \qquad [W/(cm \cdot K)]\end{aligned} \tag{54}$$

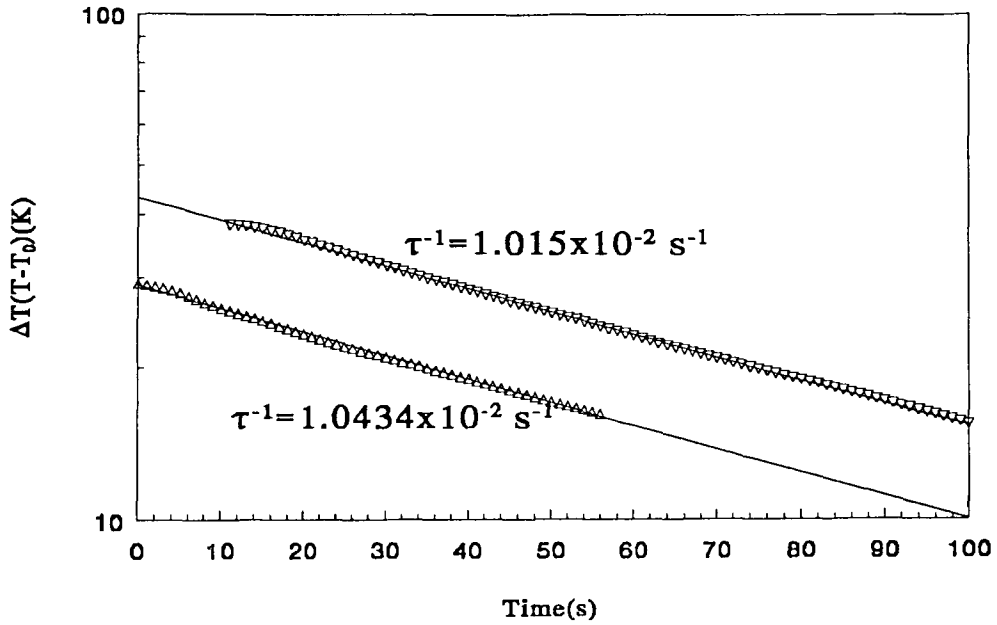

Figure 12 Temperature vs. Time due to Radiation and Conduction of Substrate.

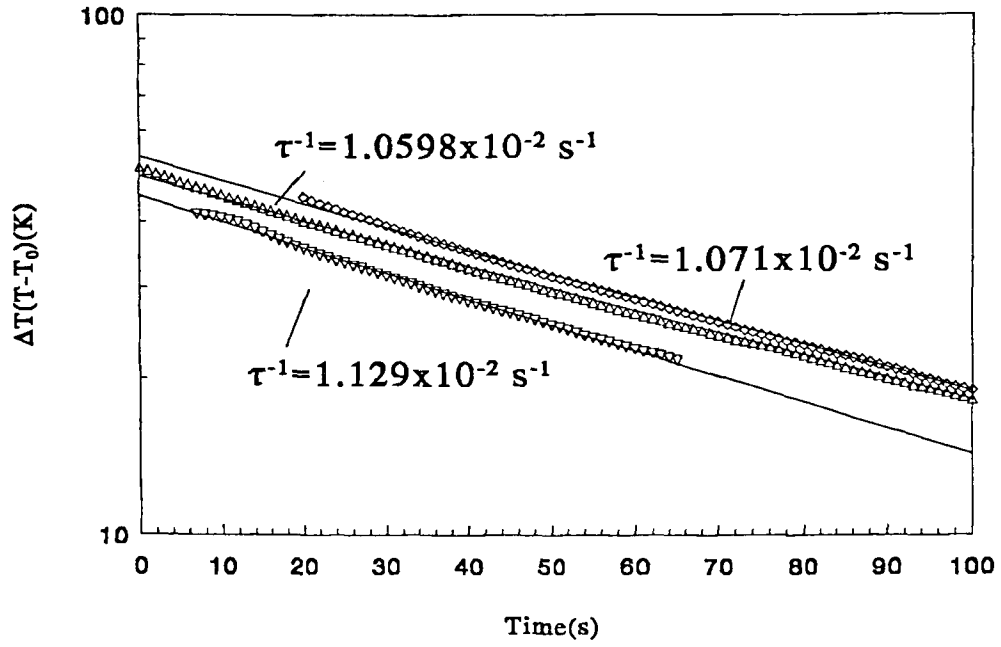

Figure 13 Temperature vs. Time due to Radiation, Conduction of Substrate and Conduction of Hard Carbon Thin Film.

This value is far below that of the natural diamond crystal [as high as 20W / (cm·K) or more]. We speculate that the quality of the film was not good enough. The films fabricated in the PACVD system is most likely not diamond crystal but polycrystal or amorphous hard carbon. It can be improved if the growing condition is better. Even that, the measured thermal conductivity of the hard carbon thin film is much better than that of the bulk SiO_2 [0.014 W / (cm·K)]. It is also much better than the thermal conductivity of amorphous carbon published in Reference [9] [0.015 W / (cm·K)].

Figure 14 is a graph that shows a group of experimental data due to different thermal transfer mechanisms.

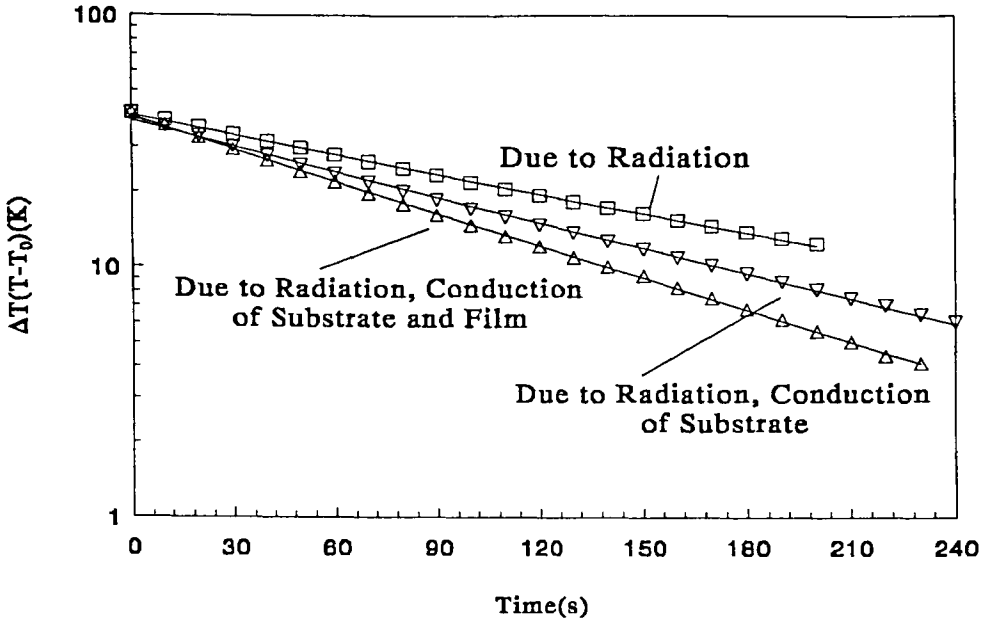

Figure 14 Measurement for Diamond-Like Film with Thickness of 2μm due to Radiation, Conduction of Substrate and Conduction of Hard Carbon Thin Film.

CHAPTER 5
CONCLUSIONS

Non-contact measurement for thermal conductivity of diamond-like and hard carbon thin films is a new method we introduced. It is a valid method for thin film with a thickness less than 2 μm, if the hard carbon thin film is deposited on a thinner glass plate. The measurement accuracy will be improve by reducing the radiation of the thermal source, i.e., shrinking the dimension of thermal source, using low temperature detector with high detectivity, keeping environment temperature and chopper temperature constant. This method can be applied not only to diamond-like and hard carbon thin films but also to films of other materials This will help us study the fabrication of thin films of high thermal conductivity.

APPENDIX A

COMPUTER(IBM 286) PROGRAM OF DATA ACQUISITION FOR THE DIAMOND THERMAL CONDUCTIVITY MEASUREMENT

```
30 DEF FNT (X) = 3600 * VAL(MID$(TIME$, 1, 2)) + 60 *
    VAL(MID$(TIME$, 4, 2)) + VAL(MID$(TIME$, 7, 2))
40 OPEN "\DEV\IEEEOUT" FOR OUTPUT AS #1      ' Open IEEE-488 output
                                               path.
50 OPEN "\DEV\IEEEIN" FOR INPUT AS #2        ' Open IEEE-488 input
                                               path.
60 IOCTL #1, "BREAK"                         ' Reset interface.
70 PRINT #1, "RESET"                         ' Warm start interface
80 PRINT #1, "CLEAR"                         ' Send device clear.
90 CLS                                       ' Clear CRT.
100 OPTION BASE 1
110 DIM T(2000), V1(2000), V2(2000)          ' Dimension reading
                                               arrays.
120 PRINT #1, "REMOTE 25"                    ' Put 195A in remote.
130 PRINT #1, "OUTPUT 25;F0X"                ' DC Volts mode.
140 PRINT #1, "OUTPUT 25;R5X"                ' 200 V Range.
150 PRINT #1, "OUTPUT 25;P1X"                ' Filter on; 64 readings
                                               averaged
160 PRINT #1, "OUTPUT 25;G1X"                ' Reading without
                                               prefix/suffix.
170 PRINT #1, "REMOTE 16"                    ' Put 195 in remote.
180 PRINT #1, "OUTPUT 16;F0X"                ' DC Volts mode.
190 PRINT #1, "OUTPUT 16;R2X"                ' 200 mV Range.
200 PRINT #1, "OUTPUT 16;P1X"                ' Filter on; 64 readings
                                               averaged.
210 PRINT #1, "OUTPUT 16;G1X"                ' Reading without
                                               prefix/suffix.
215 INPUT "SAMPLING INTERVAL (second)="; S
220 N = 1000: T0 = FNT(1)
```

```
230 FOR I = 1 TO N                          ' Loop for all N readings.
231 T$ = TIME$                              ' Check the time interval.
232 FOR K = 1 TO S
234 IF T$ = TIME$ THEN 234
235 T$ = TIME$
236 NEXT K
237 REP = 5: V1 = 0: V2 = 0
238 FOR J = 1 TO REP                        ' Average of 5 readings.
240 PRINT #1, "ENTER 25"                    ' Address 195A to talk.
250 INPUT #2, X                             ' Input Radiation density to
                                              V1(I).
260 PRINT #1, "ENTER 16"                    ' Address 195 to talk.
270 INPUT #2, Y                             ' Input thermocouple
                                              voltage readings to V2(I).
271 V1 = V1 + X: V2 = V2 + Y
272 NEXT J: V1(I) = V1 / REP: V2(I) = V2 / REP
280 T(I) = FNT(1) - T0
290 PRINT I, T(I), V1(I), V2(I)
305 IF INKEY$ = "S" THEN 320
310 NEXT I                                  ' Loop back for next
                                              reading.
320 CLOSE 1: CLOSE 2                        ' Close I/O files.
410 INPUT "DATAFILE NAME"; A$               ' Save data into disk.
420 OPEN A$ + ".DAT" FOR OUTPUT AS #1
430 FOR J = 1 TO I - 1
440 PRINT #1, T(J), V1(J), V2(J) / .00004
450 NEXT J
460 CLOSE #1
470 END
```

REFERENCES

[1] C. V. Deshpandey and R. F. Bunshah, "Diamond and Diamondlike Films: Deposition Processes and Properties", *J. Vac. Sci. Technol.* A 7(3), (1989):2294-2306.

[2] T. R. Anthony and J. L. Fleischer, "The Thermal Conductivity of Isotopically Enriched Polycrystalline Diamond Films", *J. Appl. Phys.* 69(12), (1991):8122-8125.

[3] D. T. Morelli, C. P. Beetz, and T. A. Perry, "Thermal Conductivity of Synthetic Diamond Films", *J. Appl. Phys.* 64(6), (1988):3063-3066.

[4] Y. S. Touloukian, R. W. Powell, C. Y. Ho, and P. G. Klemens, *Thermal Conductivity, Nonmetallic Solids*, IFI/Plenum, New York, (1970):202.

[5] David G. Cahill, "Thermal Conductivity Measurement from 30 to 750 K: the 3ω Method", *Rev. Sci. Instru.* 61(2), (1990):802-813.

[6] Ichiro Hatta, "Thermal Diffusivity Measurement of Thin Films by means of an AC Calorimetric Method", *Rev. Sci. Instrum.* 56(8), (1985):1643-1647.

[7] Kazuhiro Baba, Yumi Aikawa, and Nobuaki Shohata, "Thermal Conductivity of Diamond Films", *J. Appl. Phys.* 69(10), (1991):7313-7315.

[8] John David Vincent, *Fundamental of Infrared Detector Operation and Testing*, John Wiley & Sons, (1990).

[9] Robert C. Weast, et al., *CRC Handbook of Chemistry and Physics, 61st Edition*, CRC Press, (1980-1981):E-12, E-8.